# Effect of Carbide Slag on Removal of Na⁺/K⁺ from Red Mud Based on Water Leaching

Xiaofen Huang, Qin Zhang,* Wei Wang, Jingda Pan, and Yan Yang
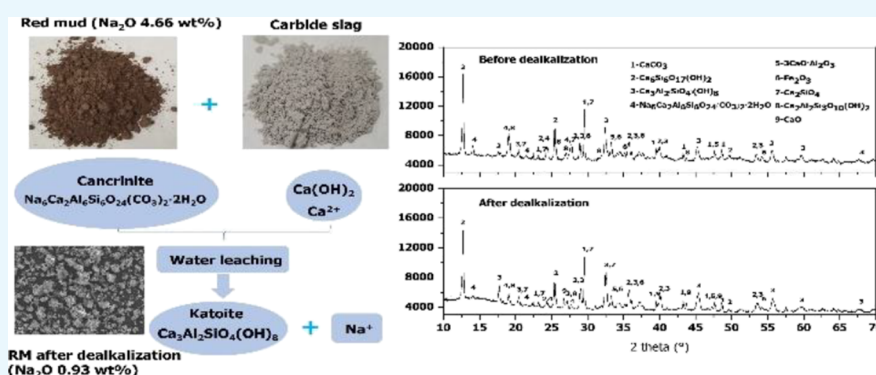
ACCESS | Metrics & More | Article Recommendations

**ABSTRACT:** Red mud (RM) is a hazardous solid waste discharged from the alumina production process. The stock of RM is very large, and it has strong alkalinity and certain radioactivity, which makes it have a very serious adverse effect on the environment. Many scholars have carried out extensive experimental investigations on the minimization, hazard-free treatment, and reutilization of RM, and encouraging results have been obtained. However, reutilization of RM has been restricted mainly due to its complex composition and strong alkalinity. In this study, carbide slag, a byproduct of acetylene production, was utilized to remove alkalis (Na⁺ and K⁺) from RM by calcium ion replacement. The effects of the temperature, liquid-to-solid ratio, carbide slag dose, and leaching time on dealkalization of RM by carbide slag were studied. The leaching mechanism of sodium was investigated and analyzed using inductively coupled plasma−atomic emission spectrometry, X-ray diffraction, and scanning electron microscopy with energy-dispersive spectrometry. Under the optimal conditions, the residual Na₂O and K₂O amount in the RM after dealkalization using the carbide slag diminished to less than 0.93 and 0.45 wt %. More than 78.80% of Na₂O and 58.84% of K₂O could be dissolved under the optimal conditions. The cancrinite structure in the initial RM was destroyed, and soluble sodium salts formed in the suspension can be easily replaced by carbide slag reducing Na⁺. The dealkalization process of RM by using carbide slag was controlled by chemical reaction of shrinking core model, where the apparent activation energy was 4.92 kJ/mol.

## 1. INTRODUCTION

Red mud (RM, bauxite residue), a byproduct of the alumina refining industry, is a type of solid waste with high alkalinity and a high heavy metal content.[1−4] For 1 t of alumina produced, approximately 1.5 t of RM is discharged.[5] In 2018, global storage of the RM reached 4.6 billion tons,[6,7] and damming disposal is still the main way to dispose of RM in the world.[8,9] RM exerts a substantial impact on environments by contaminating water and soil due to leakage of alkaline compounds, polluting the air with RM dust, and altering land occupation.[10−13] Many scholars have carried out extensive experimental investigations to find practical use for RM. For instance, RM has been suggested as a raw material for roadbed,[14,15] building,[16−18] adsorption material for environmental management such as wastewater treatment,[19,20] waste gas treatment,[21,22] and soil remediation,[23,24] and recovery of valuable metals, such as Fe, Al, Ti, Sc, and Y.[5,25−27] However, the strong alkalinity of RM restrains

its application as the raw material of waste water treatment adsorbents, fillers, and building materials. The waste water treatment adsorbents prepared from RM without dealkalization may cause secondary pollution because of the dissolution of alkali. Sodium would migrate to the material surface, resulting in the low strength and "frost" phenomenon of building materials.[28] High acid consumption and cost are also required during the leaching process of valuable metals such as titanium,[29,30] yttrium,[31] and scandium.[32]

**Table 1. Components of RM in This Study**

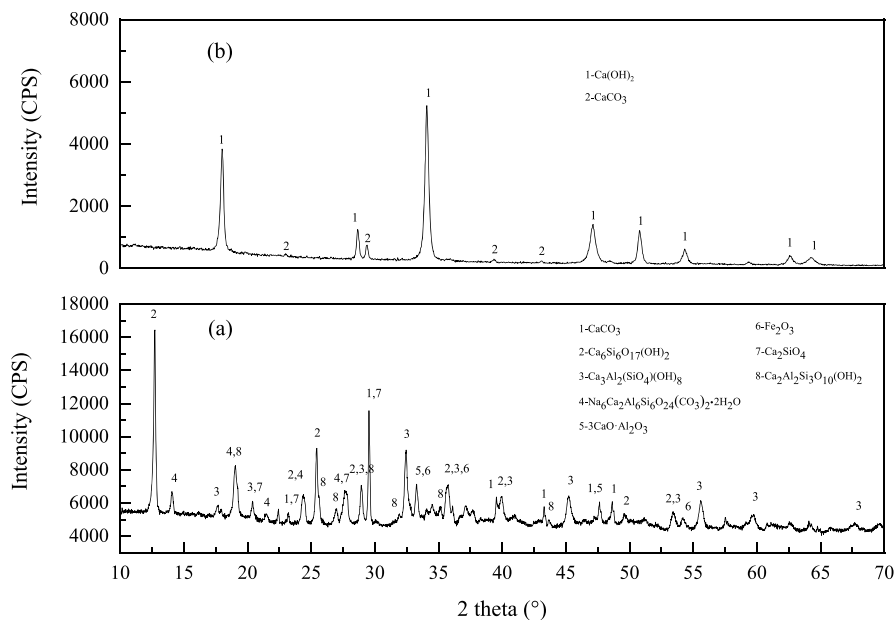| component | Na₂O | Al₂O₃ | SiO₂ | Fe₂O₃ | CaO | TiO₂ | MgO | K₂O | LOI 1000 |
|---|---|---|---|---|---|---|---|---|---|
| content (wt %) | 4.66 | 21.38 | 16.37 | 20.49 | 14.30 | 4.52 | 1.58 | 0.99 | 12.69 |



**Figure 1.** XRD pattern of the RM (a) and carbide slag (b) sample.

Meanwhile, the presence of sodium in significant quantities at alkaline pH is a significant inhibitor to the creation of the aggregate structure and hydraulic conductivities conducive to plant growth.[2,33] In addition, the presence of large concentrations of Na⁺ elevates the electrical conductivity of the solution beyond tolerable limits for plants and denies plants the uptake of water.[34] Dealkalization is a major limiting factor for the comprehensive utilization of RM. Therefore, the dealkalization process of RM is an important precondition for the next comprehensive utilization.

The pH of RM ranges over 10∼13 with an average value of 11.3 ± 1.0, which mainly depends on the production process.[35,36] At present, the main method for dealkalization of RM includes direct water leaching,[37,38] acid neutralization,[39,40] calcium ion replacement,[41−43] and wet carbonization.[44−46] Water leaching does not consume reagents, and it is inexpensive. However, the process is time-consuming, as repeated dealkalization and long-term leaching are required, and only free alkali can be removed from RM. Thus, the comprehensive use of RM subsequent to water leaching is limited. The wet carbonization method can effectively remove both free alkali and structural alkali from RM without consuming reagents. However, wet carbonization requires high pressure, strict leaching equipment requirements, and operate conditions. Acid leaching can be considered an effective dealkalization method. A large amount of Na can be leached from RM using acid leaching, but many other metallic oxides, such as iron, aluminum, and various rare metal oxides, are also dissolved by this process. Furthermore, the resulting leaching residue is difficult to apply in roadbed, building, and environmental adsorption materials due to its strong acidity. The calcium ion replacement method removes both free alkali and structural alkali from RM. Calcium ions can react with alkaline substances in RM to form tricalcium aluminate and displace sodium to reduce alkalinity, which is

conducive to the reconstruction of vegetation by improving the stability of RM microaggregates and increasing RM permeability.[47,48] Han et al.[49] demonstrated that the introduction of Ca²⁺ accelerated a pH decrease in bauxite residues while also precipitating carbonate to form calcium carbonate. Zhu[43] demonstrated that selective leaching of Na from RM was achieved using water leaching with CaO at high temperature and pressure. Cancrinite was decomposed from the RM during the selective leaching process. Liu et al.[41] treated fine RM with soda-lime roasting under reductive atmosphere prior to leaching and magnetic separation. They found that the recovery of Al and Na after the water leaching was about 75.7 and 80.7%, respectively. However, the calcium ion replacement method consumes large quantities of reagents and is therefore, expensive.

The RM dealkalization process should be economically and technologically feasible in order to achieve industrial application. Alkaline regulation by industrial waste application, achieved using the "using waste to treat waste" principle, makes RM environmental development a future possibility. It was well known that carbide slag is the byproduct of the production of acetylene using calcium carbide and its main ingredients were Ca(OH)₂ and CaCO₃.[50,51] As the main component of carbide slag is Ca(OH)₂, it is possible that carbide slag can be used in RM dealkalization. In this work, carbide slag was utilized to remove alkalis (Na⁺ and K⁺) in RM. The main factors studied were temperature, liquid-to-solid ratio (L/S), carbide slag dose, and leaching time. The leaching mechanism of sodium was investigated and analyzed using inductively coupled plasma−atomic emission spectrometry (ICP−AES), X-ray diffraction (XRD), and scanning electron microscopy with energy-dispersive spectrometry (SEM−EDS).

## 2. EXPERIMENTAL SECTION

**2.1. Materials.** The RM samples studied in this research were collected from a Bayer Process alumina plant in Guizhou Province, China. The samples were dried at 65 °C for 24 h and passed through a 60-mesh sieve prior to chemical analysis. The chemical composition of RM analyzed by X-ray fluorescence is shown in Table 1. The XRD pattern of the RM sample is shown in Figure 1.

It can be seen that the main mineral phases of the original RM were cancrinite, katoite, xonotlite, calcite, and hematite. The main minerals that caused RM to be alkaline are katoite, cancrinite, and calcite. Sodium mainly existed in cancrinite, and it was difficult to be removed using water leaching. The particle size distribution of RM is indicated in Figure 2. The size of all particles was less than 69.61 $\mu$m, while the average particle size is 9.90 $\mu$m. Therefore, leaching could be directly carried out without grinding.
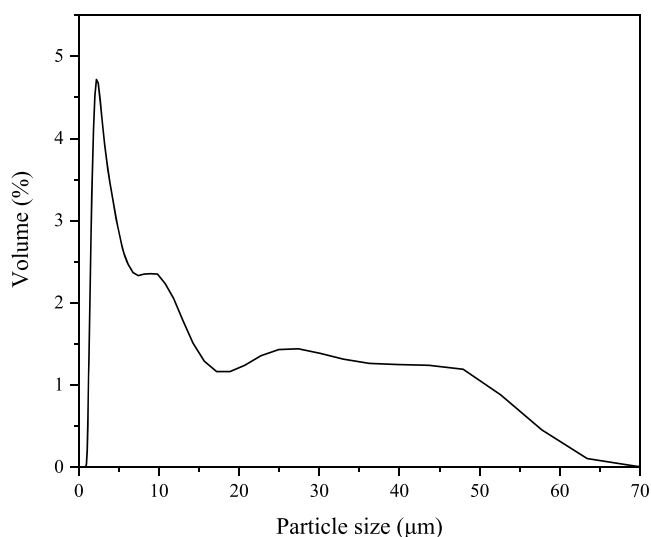


**Figure 2.** Particle size distribution of RM.

**2.2. Methods.** First, the samples of RM were dried in a DHG-9035A oven (China) at 65 °C for 12 h. Then, 10 g of the dried sample was added to some carbide slag and DI water. Three replicates of each treatment were completed in order to effectively reduce the error. The weighed RM sample (10 g) was mixed with carbide slag and 40 mL of deionized water in 250 mL bottles and sealed with a plastic membrane to prevent external interference. The ore slurry was vibrated at the speed of 160 rpm under different conditions of L/S, leaching temperature, carbide slag dosage, and leaching time by using a SHZ-88 constant temperature water bath oscillator (China). The L/S was set as 3, 4, 5, 6, and 7 (mL/g). Leaching temperature was controlled at 25, 50, 70, and 90 °C. Leaching time was set as 2, 4, 6, 8, 10, and 12 h. Carbide slag dosage was set as 5, 10, 15, 20, 25, 30, 40, and 50 wt %. The leaching solution was collected through filtration with a SHZ-D(III) vacuum suction filter (China). Then, the contents of sodium and other compositions in leaching solution were determined by ICP−AES. The leaching residue was dried at 80 °C. Then, the composition of the leaching residue was also analyzed by ICP−AES after the residue was completely decomposed in an acid solution of hydrofluoric acid, perchloric acid, and nitric acid. The dealkalization rate was calculated using eq 1

$$\eta = \frac{N}{M} \times 100\% = \frac{V \times p}{m \times q \times 10000 + V \times p} \times 100\%$$

(1)

where $\eta$ is the dealkalization rate (%), $N$ is the quantity of sodium oxide in leaching solution (g), $M$ is the quantity of sodium oxide in the RM (g), $m$ is the weight of the leaching residue (g), $q$ is the grade of sodium oxide in the RM sample (%), $V$ is the quantity of the leaching solution (mL), and $p$ is the content of sodium oxide in the leaching solution (mg/L).

**2.3. Detection and Analysis.** The $Na_2O$ and $K_2O$ contents of the RM and leaching residue were determined by ICP−AES (ICAP 7400, ThermoFisher, USA). The raw RM sample was characterized by an X-ray fluorescence analyzer (Magix PW2424, Panako, the Netherlands), X-ray powder diffraction (X Pert Powder, Panako, the Netherlands), and the particle size analyzer (LS13320, Beckman Coulter, USA). XRD was conducted with a $2\theta$ scan range from 10° to 70° at a step size of 1°/s. Patterns were indexed using Jade 6. The surface morphology and elemental distribution of the treated samples
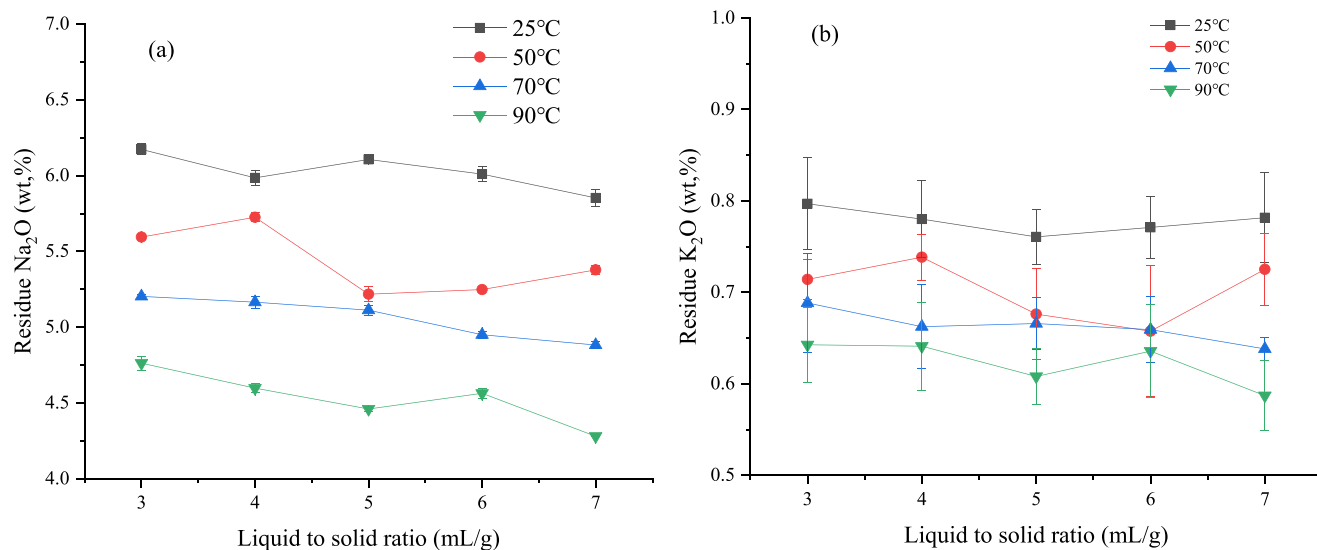


**Figure 3.** Effects of temperature and liquid-to solid ratio on dealkalization (a) Residue $Na_2O$; (b) residue $K_2O$.
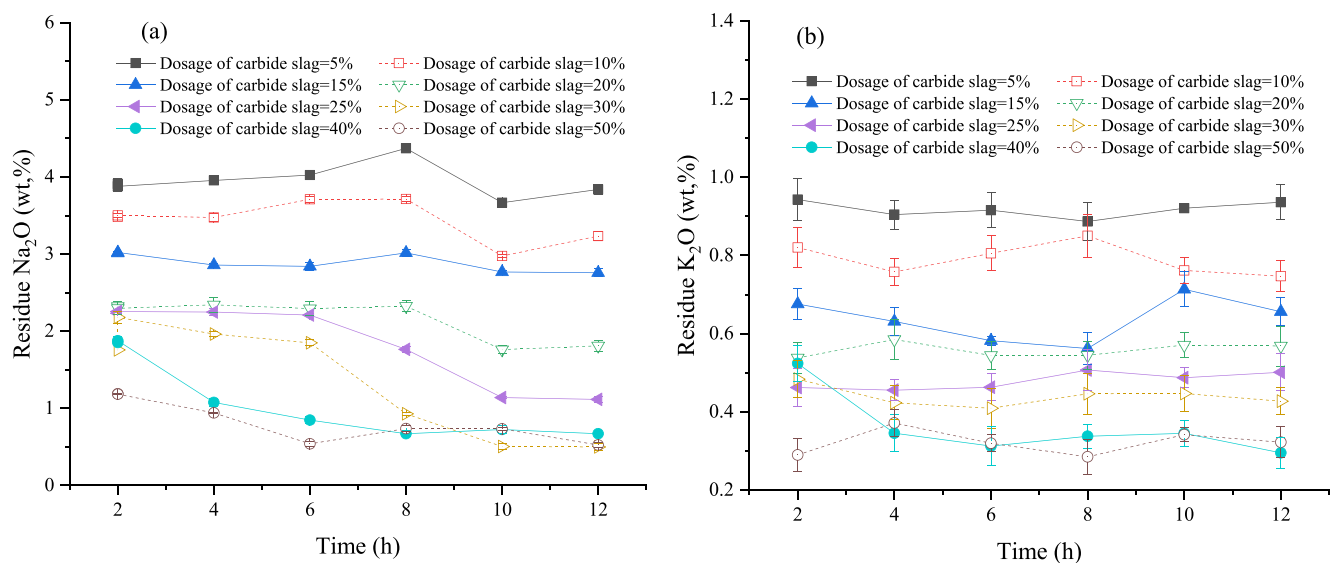
**Figure 4.** Effects of dosage of carbide slag and reaction time on dealkalization. (a) Residue $Na_2O$; (b) residue $K_2O$.
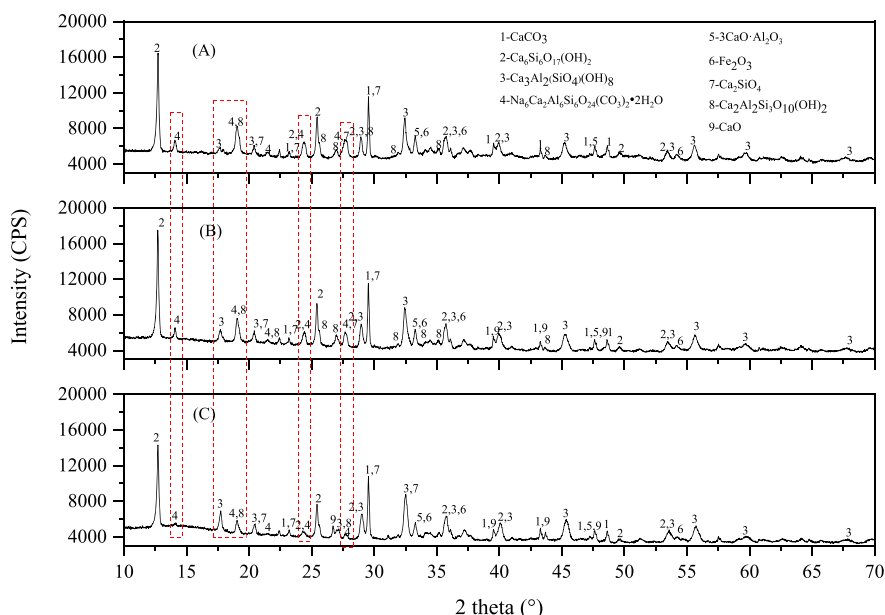


**Figure 5.** Structure changes of RM before (A) and after dealkalization by using 15 wt % carbide slag (B) and 30 wt % carbide slag (C):1-Calcite, 2-Xonotlite, 3-Katoite, 4-Cancrinite, 5-Tricalcium Aluminate, 6-Hematite, 7-Calcium silicate, 8-Prehnite, and 9-Calcium Oxide.

were analyzed by SEM−EDS (Merlin Compact, ZEISS, Germany). The thermolysis behaviors of RM samples were investigated using thermogravimetric analysis and differential scanning calorimetry (TG−DSC, 1100LF, Mettler, Switzerland).

## 3. RESULTS AND DISCUSSIONS

### 3.1. Effects of Temperature and L/S on Dealkalization.
The effect of leaching temperature and L/S on the dealkalization efficiency was investigated using 5 wt % carbide slag for 2 h. The result is shown in Figure 3, revealing that the dealkalization efficiency increased with increasing leaching temperature. The content of $Na_2O$ and $K_2O$ in the residue decreased as the temperature was increased from 25 to 90 °C. The dealkalization efficiency of both $Na_2O$ and $K_2O$ changed as the L/S increased from 3 to 7 mL/g, but not very much. Consequently, the residual alkali content in the RM is still large. Considering water

consumption and solid−liquid separation, the L/S was 3 mL/g and temperature was 90 °C.

### 3.2. Effects of Carbide Slag Dosage and Leaching Time on Dealkalization.
The effects of carbide slag dosage and leaching time on dealkalization of RM are presented in Figure 4 under the condition of leaching temperature of 90 °C and L/S of 3 mL/g. It is shown from Figure 4 that the effect of carbide slag dosage and leaching time on dealkalization rate was apparent. The residual $K_2O$ changes were not obvious with increasing leaching time. As the carbide slag dosage increased from 5 to 50 wt % for 12 h, the residual $K_2O$ decreased from 0.88 to 0.40 wt %. The residual $Na_2O$ decreased gradually with increasing carbide slag dosage and leaching time. The decrease of residual $Na_2O$ was mild at low reaction time, and it became obvious at long reaction time. The residual $Na_2O$ decreased from 3.90 to 1.19 wt % with the increasing carbide slag dosage from 5 to 50 wt % for 2 h. It decreased from 3.83 to 0.49 wt % for 12 h at the same leach
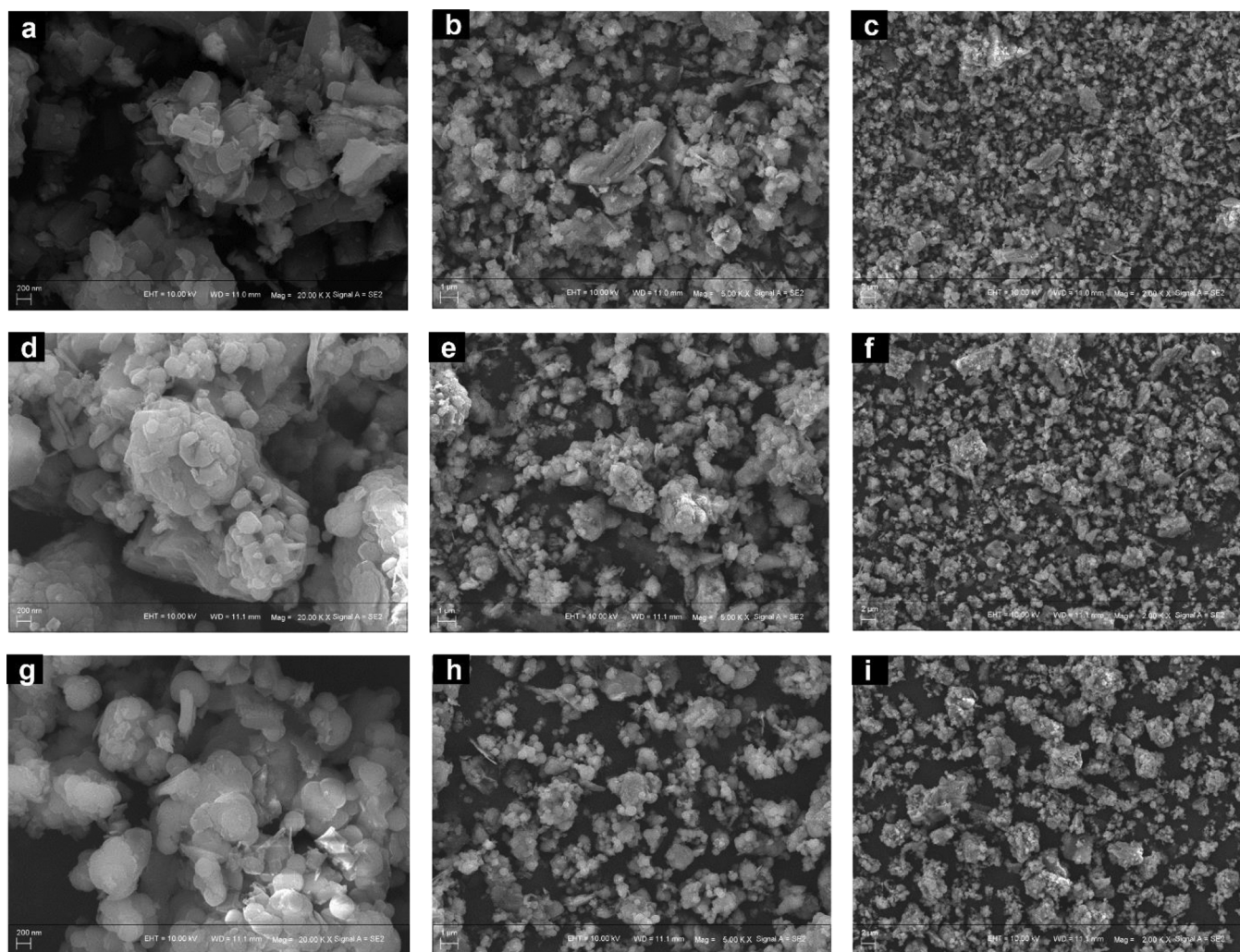
**Figure 6.** SEM photographs of initial RM (a−c), RM dealkalied by 15 wt % carbide slag (d−f), and RM dealkalied by 30 wt % carbide slag (g−i).

conditions. The residual $Na_2O$ was 2.18, 1.96, 1.84, 0.93, 0.50, and 0.49 wt % with 30 wt % carbide slag dosage for 2, 4, 6, 8, 10, and 12 h. Therefore, the suitable leaching time and carbide slag dosage were 8 h and 30 wt %, respectively. The residual $Na_2O$ in RM can be reduced to less than 1 wt % under this condition, while the dealkalization efficiencies of $Na_2O$ and $K_2O$ are 78.80 and 58.84%, respectively.

**3.3. Mechanism Analysis on Dealkalization of RM.** The mineral composition of the leaching residue was analyzed using XRD, revealing that the minerals in the leaching residue were changed after leaching with carbide slag, as shown in Figure 5. During dealkalization, calcite and hematite did not change significantly after introduction of carbide slag. In the XRD of initial RM, cancrinite is identified by the peaks at 14.0°, 19.1°, 24.4°, and 27.7°. Besides, peaks at 17.6° and 32.4° are observed for katoite. After dealkalization by carbide slag, the peaks at 14.0°, 19.1°, 24.4°, and 27.7° were weakened, indicating that the structure of cancrinite $(Na_6Ca_2Al_6Si_6O_{24}(CO_3)_2 \cdot 2H_2O)$ has been destroyed. By replacing sodium with calcium, cancrinite changed to other forms such as katoite $(Ca_3Al_2SiO_4(OH)_8)$ and Na in the form of ions is released into the solution from the RM.

The morphology and elemental distribution of the leaching residue obtained when using different carbide slag doses were analyzed using SEM−EDS, and the results are shown in Figures 6 and 7. Figure 6 shows that the particles of RM were irregular.

However, the particles became bigger and looser as the carbide slag dose was increased. The particle of RM was aggregated. It can be inferred that carbide slag can promote the agglomeration of RM particles, which is conducive to the subsequent soil remediation and secondary resource utilization of building materials.

Mapping images revealed that following carbide slag additions, Ca on the surface of RM increased, with an associated decrease in Na and K (Figure 7). According to EDS analysis, the relative mass fractions of Ca, Mg, K, and Na on the surface initial RM accounted for 3.72, 0.56, 0.82, and 4.70%, respectively. Addition of carbide slag significantly enhanced Ca, while reducing Na and K. Alkaline substances of RM are mainly divided into insoluble alkali and soluble chemical alkali. The soluble alkali is mainly composed of NaOH, $Na_2CO_3$, $NaHCO_3$, $NaAl(OH)_4$, $Na_2SiO_3$, KOH, $K_2CO_3$, and so forth,[2,7] and $Na^+$ and $K^+$ can be removed by water leaching. The insoluble alkalis are mainly composed of cancrinite, calcite, and tricalcium aluminate (TCA) in which $Na^+$ and $K^+$ are hard to remove.[36] Continuous provision of $Ca^{2+}$ by carbide slag in solution precipitates with alkaline anions and additionally exchanges sodium and potassium with insoluble alkali. Considering the XRD analysis results, the decomposition reaction of cancrinite appeared to have taken place. By replacing sodium with calcium, cancrinite changed to other forms such as katoite, and Na is
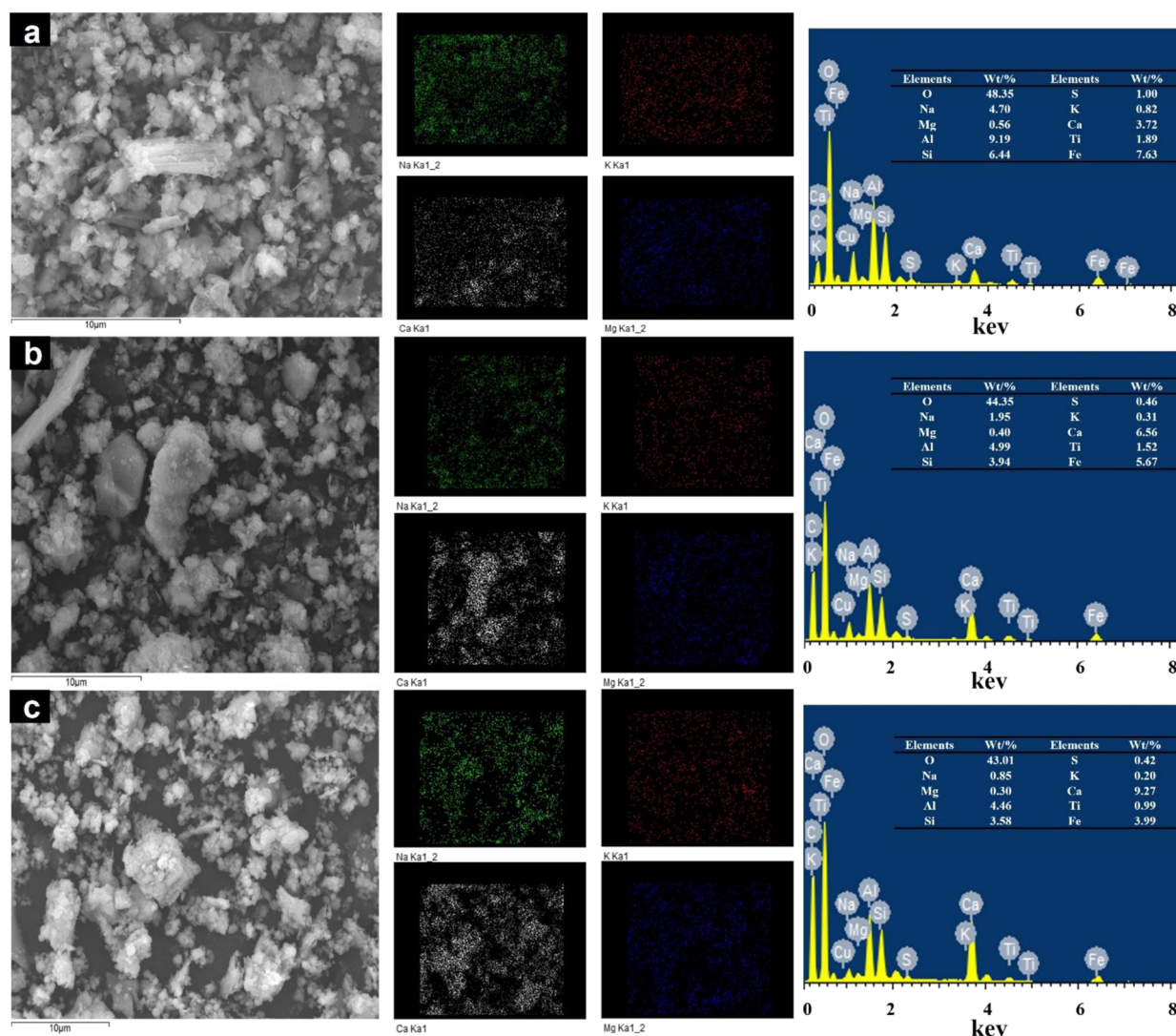
**Figure 7.** SEM−EDS image of RM before (a) and after dealkalization by 15% carbide slag (b) and after dealkalization by 30% carbide slag (c).

released into the solution from the RM. The TG−DSC curves of the initial and treated RM are depicted in Figure 8. As Figure 8 shows, the initial RM and treated RM had a similar changing trend in the thermogravimetry process.

**3.4. Leaching Kinetics of Dealkalization.** It is important to establish a quantitative measurement of the leaching kinetic to confirm the dealkalization process. The dealkalization process of RM by using carbide slag is a solid−liquid multiphase reaction, and the leaching reaction occurs at the interface of two phases. Therefore, the dealkalization process could be analyzed by the shrinking core model (SCM). According to the SCM, assuming that the leaching process is controlled by the chemical reaction, the following expression can be applied for the leaching kinetic

$$K_b t = [1 - (1 - \eta)^{1/3}] \tag{2}$$

where $\eta$ is the dealkalization rate (%), $t$ is reaction time (min), and $K_b$ is the rate constant of chemical reaction. Figure 9 was plotted according to eq 2.

According to Figure 9, the control of chemical reaction fitted the leaching data well at different temperatures. The slopes of each straight line in Figure 9 represent the reaction rate constants at different temperatures, as per the Arrhenius equation.
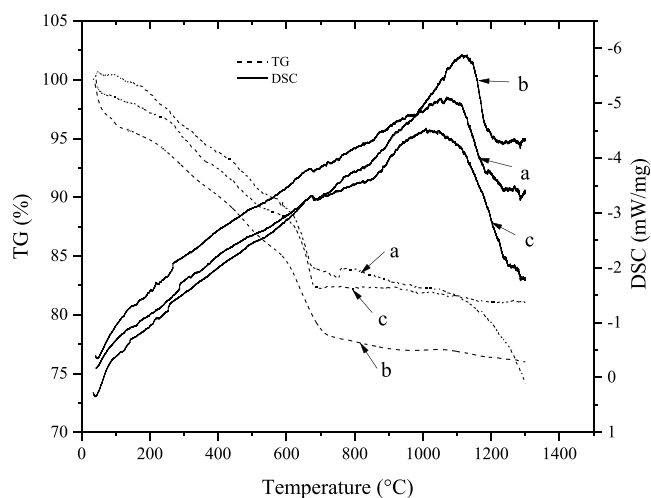


**Figure 8.** TG−DSC curve of RM before (a) and after dealkalization by 15% carbide slag (b) and after dealkalization by 30% carbide slag (c).
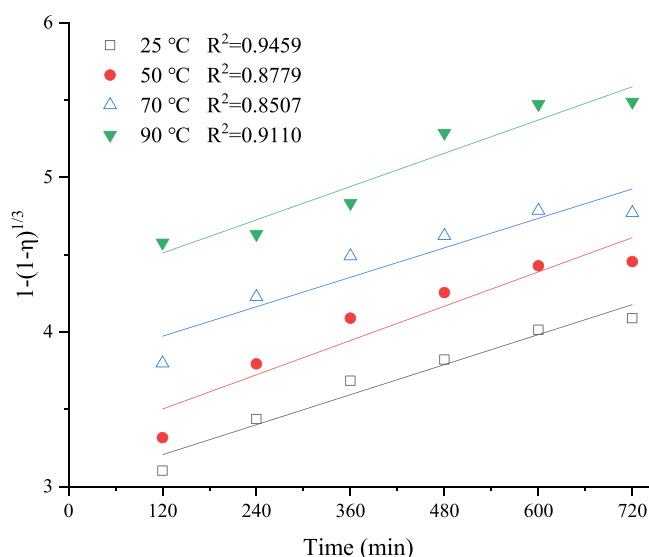
$$K_b = k_0 \exp\left(-\frac{E}{RT}\right) \tag{3}$$

**Figure 9.** Plots of $1 - (1 - \eta)^{1/3}$ vs time at different temperatures.

where $K_b$ is the reaction rate constant $(min^{-1})$, $k_0$ is the pre-exponential factor, $E$ is the apparent activation energy $(kJ \cdot mol^{-1})$, $R$ is the molar gas constant $(kJ \cdot mol^{-1} \cdot K^{-1})$, and $T$ is the thermodynamic temperature (K). The Arrhenius curve is plotted in Figure 10, with $1/T$ and $\ln K_b$ as the horizontal and vertical ordinates, respectively; the apparent activation energy $E$ was calculated as $4.92$ kJ·mol$^{-1}$.



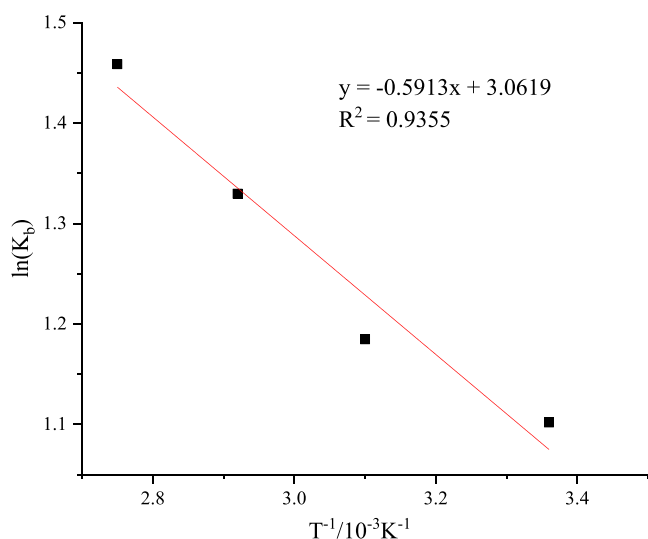$$y = -0.5913x + 3.0619$$
$$R^2 = 0.9355$$

**Figure 10.** Plot of $\ln K_b$ vs temperature of leaching.

## 4. CONCLUSIONS

The results obtained in the present work showed that the alkalis could be obviously removed using water leaching with carbide slag. The carbide slag dose, temperature, and leaching time were found to be a key factor determining the dealkalization efficiency according to the results of the dealkalization experiments. When the carbide slag dosage was 30 wt %, the leaching time was 8 h, temperature was 90 °C, and L/S was 3 mL/g, and the results showed that dealkalization efficiencies of $Na_2O$ and $K_2O$ were 78.80 and 58.84%, respectively, and the residual $Na_2O$ and $K_2O$ were 0.93 and 0.45 wt %, respectively. The mineral cancrinite

$(Na_6Ca_2Al_6Si_6O_{24}(CO_3)_2 \cdot 2H_2O)$ was decomposed in the leaching process. By replacing sodium with calcium, cancrinite changed to other forms such as katoite $(Ca_3Al_2SiO_4(OH)_8)$, and Na in the form of ions is released into the solution from the RM. The dealkalization process of RM by using carbide slag was controlled by chemical reaction of SCM, where the apparent activation energy was 4.92 kJ/mol.

## ■ AUTHOR INFORMATION

### Corresponding Author

**Qin Zhang** − *Guizhou Academy of Science, Guiyang 550001 Guizhou, China; National & Local Joint Laboratory of Engineering for Effective Utilization of Regional Mineral Resources from Karst Areas, Guiyang 550025 Guizhou, China; Guizhou Key Laboratory of Comprehensive Utilization of Non-metallic Mineral Resources, Guiyang 550025 Guizhou, China;* orcid.org/0000-0003-1253-8652; Email: zq6736@163.com

### Authors

**Xiaofen Huang** − *College of Resources and Environmental Engineering, Guizhou University, Guiyang 550025 Guizhou, China; National & Local Joint Laboratory of Engineering for Effective Utilization of Regional Mineral Resources from Karst Areas, Guiyang 550025 Guizhou, China; Guizhou Key Laboratory of Comprehensive Utilization of Non-metallic Mineral Resources, Guiyang 550025 Guizhou, China;* orcid.org/0000-0003-3612-0824

**Wei Wang** − *College of Mining, Guizhou University, Guiyang 550025, China*

**Jingda Pan** − *College of Mining, Guizhou University, Guiyang 550025, China*

**Yan Yang** − *College of Mining, Guizhou University, Guiyang 550025, China*

Complete contact information is available at:
https://pubs.acs.org/10.1021/acsomega.1c05600

### Notes

The authors declare no competing financial interest.

## ■ REFERENCES

(1) Archambo, M.; Kawatra, S. K. Red Mud: Fundamentals and New Avenues for Utilization. *Miner. Process. Extr. Metall. Rev.* **2021**, *42*, 427−450.

(2) Gräfe, M.; Power, G.; Klauber, C. Bauxite residue issues: III Alkalinity and associated chemistry. *Hydrometallurgy* **2011**, *108*, 60−79.

(3) Power, G.; Gräfe, M.; Klauber, C. Bauxite residue issues: I. Current management, disposal and storage practices. *Hydrometallurgy* **2011**, *108*, 33−45.

(4) Zhu, F.; Liao, J.; Xue, S.; Hartley, W.; Zou, Q.; Wu, H. Evaluation of aggregate microstructures following natural regeneration in bauxite residue as characterized by synchrotron-based X-ray micro-computed tomography. *Sci. Total Environ.* **2016**, *573*, 155−163.

(5) Wang, L.; Sun, N.; Tang, H.; Sun, W. A Review on Comprehensive Utilization of Red Mud and Prospect Analysis. *Minerals* **2019**, *9*, 362.

(6) Tian, T.; Zhou, J.; Zhu, F.; Ye, Y.; Guo, Y.; Hartley, W.; Xue, S. Effect of amendments on the leaching behavior of alkaline anions and metal ions in bauxite residue. *J. Environ. Sci.* **2019**, *85*, 74−81.

(7) Xue, S.; Wu, Y.; Li, Y.; Kong, X.; Zhu, F.; William, H.; Li, X.; Ye, Y. Industrial wastes applications for alkalinity regulation in bauxite residue: A comprehensive review. *J. Cent. South Univ.* **2019**, *26*, 268−288.

(8) Rai, S.; Bahadure, S.; Chaddha, M. J.; Agnihotri, A. Disposal Practices and Utilization of Red Mud (Bauxite Residue): A Review in Indian Context and Abroad. *J. Sustainable Metall.* **2020**, *6*, 1−8.

(9) Wang, S.; Jin, H.; Deng, Y.; Xiao, Y. Comprehensive utilization status of red mud in China: A critical review. *J. Cleaner Prod.* **2021**, *289*, No. 125136.

(10) Howe, P. L.; Clark, M. W.; Reichelt-Brushett, A.; Johnston, M. Toxicity of raw and neutralized bauxite refinery residue liquors to the freshwater cladoceran Ceriodaphnia dubia and the marine amphipod Paracalliope australis. *Environ. Toxicol. Chem.* **2011**, *30*, 2817−2824.

(11) Mayes, W. M.; Burke, I. T.; Gomes, H. I.; Anton, Á. D.; Molnár, M.; Feigl, V.; Ujaczki, É. Advances in Understanding Environmental Risks of Red Mud After the Ajka Spill, Hungary. *J. Sustainable Metall.* **2016**, *2*, 332−343.

(12) Mukiza, E.; Zhang, L.; Liu, X.; Zhang, N. Utilization of red mud in road base and subgrade materials: A review. *Resour., Conserv. Recycl.* **2019**, *141*, 187−199.

(13) Reddy, P. S.; Reddy, N. G.; Serjun, V. Z.; Mohanty, B.; Das, S. K.; Reddy, K. R.; Rao, B. H. Properties and Assessment of Applications of Red Mud (Bauxite Residue): Current Status and Research Needs. *Waste Biomass Valoriz.* **2021**, *12*, 1185−1217.

(14) Chen, R.; Cai, G.; Dong, X.; Mi, D.; Puppala, A. J.; Duan, W. Mechanical properties and micro-mechanism of loess roadbed filling using by-product red mud as a partial alternative. *Constr. Build. Mater.* **2019**, *216*, 188−201.

(15) Li, Y.; Liu, X.; Li, Z.; Ren, Y.; Wang, Y.; Zhang, W. Preparation, characterization and application of red mud, fly ash and desulfurized gypsum based eco-friendly road base materials. *J. Cleaner Prod.* **2021**, *284*, No. 124777.

(16) He, H.; Yue, Q.; Su, Y.; Gao, B.; Gao, Y.; Wang, J.; Yu, H. Preparation and mechanism of the sintered bricks produced from Yellow River silt and red mud. *J. Hazard. Mater.* **2012**, *203−204*, 53−61.

(17) Kim, S. Y.; Jun, Y.; Jeon, D.; Oh, J. E. Synthesis of structural binder for red brick production based on red mud and fly ash activated using Ca(OH)2 and Na2CO3. *Constr. Build. Mater.* **2017**, *147*, 101−116.

(18) Li, X.; Zhang, Q.; Mao, S. Investigation of the bond strength and microstructure of the interfacial transition zone between cement paste and aggregate modified by Bayer red mud. *J. Hazard. Mater.* **2021**, *403*, No. 123482.

(19) Wu, W.; Chen, Z.; Huang, Y.; Li, J.; Chen, D.; Chen, N.; Su, M. Red mud for the efficient adsorption of U(VI) from aqueous solution: Influence of calcination on performance and mechanism. *J. Hazard. Mater.* **2021**, *409*, No. 124925.

(20) Wang, L.; Hu, G.; Lyu, F.; Yue, T.; Tang, H.; Han, H.; Yang, Y.; Liu, R.; Sun, W. Application of Red Mud in Wastewater Treatment. *Minerals* **2019**, *9*, 281.

(21) Yang, W.; Hussain, A.; Zhang, J.; Liu, Y. Removal of elemental mercury from flue gas using red mud impregnated by KBr and KI reagent. *Chem. Eng. J.* **2018**, *341*, 483−494.

(22) Apeksha, M.; Rajanikanth, B. S. Plasma/adsorbent system for NOx treatment in diesel exhaust: a case study on solid industrial wastes. *Int. J. Environ. Sci. Technol.* **2019**, *16*, 2973−2988.

(23) Hua, Y.; Heal, K. V.; Friesl-Hanl, W. The use of red mud as an immobiliser for metal/metalloid-contaminated soil: A review. *J. Hazard. Mater.* **2017**, *325*, 17−30.

(24) Joseph, C. G.; Taufiq-Yap, Y. H.; Krishnan, V.; Puma, G. L. Application of modified red mud in environmentally-benign applications: A review paper. *Environ. Eng. Res.* **2020**, *25*, 795−806.

(25) Samal, S. Utilization of Red Mud as a Source for Metal Ions—A Review. *Materials* **2021**, *14*, 2211.

(26) Zhang, X.; Zhou, K.; Chen, W.; Lei, Q.; Huang, Y.; Peng, C. Recovery of iron and rare earth elements from red mud through an acid leaching-stepwise extraction approach. *J. Cent. South Univ.* **2019**, *26*, 458−466.

(27) Zhou, K.; Teng, C.; Zhang, X.; Peng, C.; Chen, W. Enhanced selective leaching of scandium from red mud. *Hydrometallurgy* **2018**, *182*, 57−63.

(28) Kang, S.; Kwon, S. Effects of red mud and Alkali-Activated Slag Cement on efflorescence in cement mortar. *Constr. Build. Mater.* **2017**, *133*, 459−467.

(29) Agatzini-Leonardou, S.; Oustadakis, P.; Tsakiridis, P. E.; Markopoulos, C. Titanium leaching from red mud by diluted sulfuric acid at atmospheric pressure. *J. Hazard. Mater.* **2008**, *157*, 579−586.

(30) Huang, Y.; Chai, W.; Han, G.; Wang, W.; Yang, S.; Liu, J. A perspective of stepwise utilisation of Bayer red mud: Step two– Extracting and recovering Ti from Ti-enriched tailing with acid leaching and precipitate flotation. *J. Hazard. Mater.* **2016**, *307*, 318−327.

(31) Rivera, R. M.; Xakalashe, B.; Ounoughene, G.; Binnemans, K.; Friedrich, B.; Van Gerven, T. Selective rare earth element extraction using high-pressure acid leaching of slags arising from the smelting of bauxite residue. *Hydrometallurgy* **2019**, *184*, 162−174.

(32) Zhu, X.; Niu, Z.; Li, W.; Zhao, H.; Tang, Q. A novel process for recovery of aluminum, iron, vanadium, scandium, titanium and silicon from red mud. *J. Environ. Chem. Eng.* **2020**, *8*, No. 103528.

(33) Xue, S.; Zhu, F.; Kong, X.; Wu, C.; Huang, L.; Huang, N.; Hartley, W. A review of the characterization and revegetation of bauxite residues (Red mud). *Environ. Sci. Pollut. Res.* **2016**, *23*, 1120−1132.

(34) Gräfe, M.; Klauber, C. Bauxite residue issues: IV. Old obstacles and new pathways for in situ residue bioremediation. *Hydrometallurgy* **2011**, *108*, 46−59.

(35) Jones, B. E. H.; Haynes, R. J. Bauxite Processing Residue: A Critical Review of Its Formation, Properties, Storage, and Revegetation. *Crit. Rev. Environ. Sci. Technol.* **2011**, *41*, 271−315.

(36) Lyu, F.; Hu, Y.; Wang, L.; Sun, W. Dealkalization processes of bauxite residue: A comprehensive review. *J. Hazard. Mater.* **2021**, *403*, No. 123671.

(37) Liu, Z.; Li, H.; Huang, M.; Jia, D.; Zhang, N. Effects of cooling method on removal of sodium from active roasting red mud based on water leaching. *Hydrometallurgy* **2017**, *167*, 92−100.

(38) Zhu, X.; Li, W.; Guan, X. An active dealkalization of red mud with roasting and water leaching. *J. Hazard. Mater.* **2015**, *286*, 85−91.

(39) Li, W.; Zhu, X.; Tang, S. Selective separation of sodium from red mud with citric acid leaching. *Sep. Sci. Technol.* **2017**, *52*, 1876−1884.

(40) Peng, H.; Kim, T.; Vaughan, J. Acid Leaching of Desilication Products: Implications for Acid Neutralization of Bauxite Residue. *Ind. Eng. Chem. Res.* **2020**, *59*, 8174−8182.

(41) Liu, W.; Sun, S.; Zhang, L.; Jahanshahi, S.; Yang, J. Experimental and simulative study on phase transformation in Bayer red mud soda-lime roasting system and recovery of Al, Na and Fe. *Miner. Eng.* **2012**, *39*, 213−218.

(42) Xue, S.; Kong, X.; Zhu, F.; Hartley, W.; Li, X.; Li, Y. Proposal for management and alkalinity transformation of bauxite residue in China. *Environ. Sci. Pollut. Res.* **2016**, *23*, 12822−12834.

(43) Zhu, X.; Li, W.; Zhao, H.; Zhang, C. Selective Dealkalization of Red Mud Using Calcium Oxide with Pressure Leaching. *Jom* **2018**, *70*, 2800−2806.

(44) Jones, G.; Joshi, G.; Clark, M.; McConchie, D. Carbon capture and the aluminium industry. Preliminary studies. *Environ. Chem.* **2007**, *3*, 297−303.

(45) Khaitan, S.; Dzombak, D. A.; Lowry, G. V. Mechanisms of Neutralization of Bauxite Residue by Carbon Dioxide. *J. Environ. Eng.* **2009**, *135*, 433−438.

(46) Lu, G.; Zhang, T.; Ma, L.; Wang, Y.; Zhang, W.; Zhang, Z.; Wang, L. Utilization of Bayer red mud by a calcification−carbonation method using calcium aluminate hydrate as a calcium source. *Hydrometallurgy* **2019**, *188*, 248−255.

(47) Lehoux, A. P.; Lockwood, C. L.; Mayes, W. M.; Stewart, D. I.; Mortimer, R. J.; Gruiz, K.; Burke, I. T. Gypsum addition to soils contaminated by red mud: implications for aluminium, arsenic, molybdenum and vanadium solubility. *Environ. Geochem. Health* **2013**, *35*, 643−656.

(48) Xue, S.; Li, X.; Kong, X.; Wu, C.; Li, Y.; Li, M.; Li, C. Alkaline regulation of bauxite residue: A comprehensive review. *Huanjing Kexue Xuebao* **2017**, *37*, 2815−2828.

(49) Han, Y. S.; Ji, S.; Lee, P. K.; Oh, C. Bauxite residue neutralization with simultaneous mineral carbonation using atmospheric CO2. *J. Hazard. Mater.* **2017**, *326*, 87−93.

(50) Gu, X.; Tan, H.; He, X.; Smirnova, O.; Zhang, J.; Luo, Z. Utilization of Carbide Slag by Wet Grinding as an Accelerator in Calcium Sulfoaluminate Cement. *Materials* **2020**, *13*, 4526.

(51) Yang, B.; Shao, Z.; Zhang, D.; Wang, B. A mild route for the preparation of calcium carbonate rod bundles in large scale from carbide slag. *Micro Nano Lett.* **2021**, *16*, 187−193.